Journal of Cleaner Production 362 (2022) 132482

Contents lists available at ScienceDirect

Journal of Cleaner Production

journal homepage: www.elsevier.com/locate/jclepro

Dissolution behavior of DTPA-promoted barium slag and synthesis of submicron $BaSO_4$ particles

Tengfei Guo [a,b], Hannian Gu [a,b,*], Ning Wang [a]

[a] Key Laboratory of High-temperature and High-pressure Study of the Earth's Interior, Institute of Geochemistry, Chinese Academy of Sciences, Guiyang, 550081, China
[b] University of Chinese Academy of Sciences, Beijing, 100049, China

ARTICLE INFO

Handling Editor: Zhen Leng

Keywords:
Barium slag
DTPA
Complexation and decomplexation
Submicron $BaSO_4$ particles

ABSTRACT

Barium slag (BS) is a kind of industrial solid waste generated in barium salt production. Barium in BS can be considered as a secondary source as the content of BaO is as high as 34.80%. The main existent forms of barium in BS are $BaSO_4$, $BaCO_3$ and $BaSiO_3$. It is challenging to dissolve $BaSO_4$ using conventional acids and alkalis due to the low solubility. In this study, diethylenetriaminepentaacetic acid (DTPA) was introduced to investigate the dissolution behavior of barium in BS, and the DTPA complex solution was acidified to release barium for submicron $BaSO_4$ products preparation. Leaching tests were carried out at DTPA concentrations of 0.025–0.30 mol/L, liquid solid ratio of 10–100 mL/g, pH of 8.0–13.0, and reaction temperature of 20–80 °C. The leaching efficiency of barium was 78.64% under the conditions of using 0.10 mol/L DTPA solution (pH of 12.0) at 80 °C for 300 min with the liquid solid ratio of 50 mL/g. $BaSO_4$ products were obtained by the addition of H_2SO_4 to acidify the leachate at pH ranges of 9.0–7.5. Characterization results from X-ray diffraction, scanning electron microscopy, transmission electron microscopy and dynamic light scattering indicated that the $BaSO_4$ products were nearly sphere particles with the average diameter of 300–500 nm. This work demonstrates that DTPA can dissolve barium in BS and acidifying Ba-DTPA leachate can dissociate barium ions. Furthermore, barium source in BS can be recovered in the form of submicron $BaSO_4$ products through DTPA complexation and decomplexation process.

1. Introduction

Barium slag (BS) is a kind of industrial solid waste discharged during the refining of barite by the process of carbothermal reduction (Salem and Jamshidi, 2012). In the productive process of barium salt, barite is reduced to barium sulfide by coke or coal in a rotary kiln at about 1100 °C (Jamshidi and Ale Ebrahim, 2008; Salem and Osgouei, 2009). Barium sulfide dissolves in hot water and subsequently reacts with corresponding reagents (e.g., Na_2SO_4, Na_2CO_3 and HCl) to produce various barium products (Guzmán et al., 2012). Meanwhile, the insoluble impurities after water filtration are BS wastes. As reported, producing each ton of barium salt product can generate approximately 0.8–1.0 ton of BS (Guo et al., 2020). In China, about 1.0 million ton of BS is discharged annually and quantities of BS are accumulated (Chen et al., 2021; Xie et al., 2021). BS is classified as hazardous waste owing to its highly alkaline and high content of soluble barium ions (Gu et al., 2019; Huang et al., 2022). At present, the common disposal of BS is landfilling, and it would lead to considerable negative environmental impacts on soil, water, air, and plants, ultimately threatening human health throughout the food chain (Menzie et al., 2008; Vaidya et al., 2010; Lu et al., 2019). Therefore, it is necessary to develop new methods to dispose of BS and reduce environmental pollution.

BS mainly consists of unreacted barite, coal or coke, barium carbonate, barium sulfide, and silica (Yang et al., 2021). For the value-added utilization of BS, researchers have taken an interest in the application of BS as adsorbents and cement clinker materials. It has been reported that BS can be applied to remove hexavalent chromium (Ding, 2005), sulfate (Mulopo and Motaung, 2014), and phosphate (Guo et al., 2020) in the wastewater. BS contains certain potential cementitious minerals and alkali-earth metals components that can be used as alkaline activator (Huang et al., 2022). Due to this reason, BS shows high gelling properties and good activation effects (Jiang, 2007). Recently, BS was reported to use as a supplementary cementitious material (Chen et al., 2021), an admixture in alkali activated slag cement (Huang et al.,

* Corresponding author. Key Laboratory of High-temperature and High-pressure Study of the Earth's Interior, Institute of Geochemistry, Chinese Academy of Sciences, Guiyang, 550081, China.
E-mail address: guhannian@vip.gyig.ac.cn (H. Gu).

https://doi.org/10.1016/j.jclepro.2022.132482
Received 15 January 2022; Received in revised form 19 April 2022; Accepted 28 May 2022
Available online 30 May 2022

2022), and a raw material for sulfoaluminate clinker (Zhu et al., 2021; He et al., 2022) and for BS building bricks (Liu et al., 2017). BS can only be used for preparing non-load-bearing bricks for the high content of barium inside makes the bricks heavy. In addition, various attempts have been made to recycle and utilize resources in BS for its high contents of barium and carbon. Yang et al. (2021) reported that carbon resources in BS can be recovered through forth flotation. Acid leaching and chlorination roasting-water leaching processes were undertaken to recycle the barium resources in BS (Dong et al., 2003; Shang et al., 2021). However, the high acid consumption and low recovery lead to strong corrosive contamination; thus, these technologies have not been used widely. Recovery of barium from BS can recycle the barium resource to reduce waste of barium, and can also decrease the emissions of BS. Furthermore, if the barium-bearing components with high densities were separated or recovered, the residual BS is expected to be widely used in building wall bricks.

Diethylenetriaminepentaacetic acid (DTPA) is a common organic chelating agent, which has been widely applied to remove barite and calcite scale from oil pipelines due to its strong chelating ability (Fredd and Fogler, 1998; Dunn and Yen, 1999; Bageri et al., 2017a). In terms of barite dissolution, DTPA has a better dissolution capacity than other polyaminocarboxylic compounds, e.g., ethylenedinitrilotetraacetic acid (EDTA) (Bageri et al., 2017b). The mechanism and kinetics of barite-DTPA interactions have been investigated (Putnis et al., 2008; Kowacz et al., 2009), and its application in the petroleum industry to dissolve $BaSO_4$ precipitates as a scale or to remove barite filter cake has been reported (Bageri et al., 2017a, 2017b; Abib et al., 2018). Barite is usually the dominant mineral phase in BS, and dissolution of barite can realize a high Ba recovery. With this in mind, the current study aims to reveal the dissolution of Ba-bearing substances (mainly as barium sulfate) in BS using DTPA solution to recycle Ba as valuable resources. Meanwhile, the dissolution behavior of barium and calcium was compared since calcium in BS can also be dissolved (Kowacz et al., 2009). The dissolution tests were performed to optimize leaching conditions including concentration, liquid solid ratio, pH, temperature and reaction time. Finally, submicron $BaSO_4$ particles were synthesized from the Ba-DTPA complex solution exploiting the differences of complexation capacity between Ba-DTPA and Ca-DTPA at different pH values, and the Ba-DTPA decomplexation behavior was investigated at different pH values.

2. Materials and methods

2.1. Samples and reagents

The BS sample used in this study was collected from Guizhou Tianzhu Chemical Co., Ltd., Guizhou, China. Before analysis and leaching tests, the BS was dried to a constant weight and then crushed using a mortar and pestle until the particles ground into less than 75 μm. DTPA (98%) was used for the leaching process to dissolve barium in this study, KOH and H_2SO_4 (95.0–98.0 wt/v %) were used to adjust the pH of solutions. All the reagents used are analytical grades, and the solutions were prepared using deionized water.

2.2. Experimental procedures

2.2.1. BS dissolution using DTPA solution

A series of tests were performed to investigate the effect of different experimental parameters and to determine the optimum dissolution conditions. All the dissolution experiments were carried out using 2.0 g of BS in conical flasks which were placed in a water-bathing constant temperature vibrator with an agitation of 200 rpm. DTPA was dissolved in deionized water with the addition of KOH for pH adjustment to prepare a standard 0.5 mol/L DTPA solution. According to the previous literatures (Bageri et al., 2017a; Abib et al., 2018) and our preliminary experiments, batch leaching experimental conditions were determined as follows. To investigate the effect of DTPA concentration, the standard solution was diluted to make the corresponding concentrations, and the final pH of the solution was maintained at 12.0 by adding KOH. Leaching reactions with different concentrations (0.025, 0.05, 0.10, 0.20 and 0.30 mol/L) were performed at the conditions of using different DTPA concentrations for 300 min with a liquid solid ratio of 50 mL/g at 80 °C. The reaction temperature (20, 40, 60 and 80 °C) and pH (8.0, 9.0, 10.0, 11.0, 12.0 and 13.0) trials were conducted in 100 mL of 0.10 mol/L DTPA solutions for 300 min. In addition, the liquid solid ratio (10, 25, 50, 75 and 100 mL/g) and leaching time (10, 30, 60, 120, 180, 300 and 720 min) were also studied using 0.10 mol/L DTPA with pH of 12.0 at 80 °C to obtain the optimum conditions. After the reaction, the supernatant solutions (Ba-DTPA leachates) were filtered through 0.45 μm membranes and the concentrations of Ba and Ca were detected by ICP-AES. All the above leaching experiments were performed in triplicate.

To sum up the above results, the leaching efficiencies of barium and calcium ions were evaluated by the following equation (1):

$$\varepsilon\ (\%) = \frac{V^* c}{m^* w} * 100 \tag{1}$$

where ϵ (%) indicates the leaching efficiency of Ba or Ca; V (L) is the total solution volume; c (g/L) represents the concentration of Ba or Ca in the solution; m (g) is the mass of the BS materials used; and w (%) is the Ba or Ca content in the original BS.

2.2.2. $BaSO_4$ particles precipitation

To investigate the decomplexation behavior of Ba-DTPA solution and morphology transition process of barium sulfate precipitated, hydrochloric/sulfuric acid was used to acidify the solution to different pH values. The Ba-DTPA leachate used for decomplexation was obtained under the conditions of using 0.10 mol/L DTPA (pH = 12.0) at 80 °C for 300 min with a liquid solid ratio of 50 mL/g. During the process of $BaSO_4$ precipitating, 50 mL of the above leachates were placed in a beaker and 2 mol/L of H_2SO_4 was added dropwise to each of the solutions until the pH reached the corresponding values (pH of 9.0, 8.5 and 7.5) at room temperature. When each set pH value achieved for several minutes, the solution gradually turned to be turbid. Subsequently, white pasty precipitates were produced, and the solution was left to stand for 12 h to ensure a complete reaction. Finally, the precipitates were centrifuged from the solution and washed two times with deionized water. After drying at 60 °C for 24 h, $BaSO_4$ products were obtained.

2.3. Characterization and analysis

X-ray fluorescence spectroscopy (XRF, PANalytical Empyrean, Netherlands) was used to determine the main chemical compositions of BS. The concentrations of barium ions and calcium ions were analyzed by inductively coupled plasma-atomic emission spectrometry (ICP-AES, Agilent VISTA, USA). A prepared sample was dissolved in aqua regia, diluted to a certain volume, and then determined using ICP-AES. The mineral compositions of BS and subsequent synthesized barium sulfate particles were identified by an X-ray diffractometer (XRD, PANalytical Empyrean, Netherlands). Fourier transform infrared (FTIR, VERTEX 70, Brock, Germany) spectroscopy method was used to investigate the functional groups of the barium sulfate particles. Scanning electron microscopy (SEM, JSM-7800F, Japan) and transmission electron microscope equipped with EDS (TEM, Tecnai G2 F20 S-Twin, USA) were used for morphological observation and component analysis of the synthesized $BaSO_4$ particles. The diameter distribution of the obtained $BaSO_4$ products was examined by dynamic light scattering (DLS, NanoBrook Omni, USA).

Table 1
Main chemical composition of BS (wt %).

Components	Al_2O_3	BaO	CaO	Fe_2O_3	K_2O	MgO	P_2O_5	SiO_2	SO_3	SrO	LOI
BS	2.15	34.80	11.20	1.51	0.61	3.72	0.49	20.46	8.80	0.19	14.95

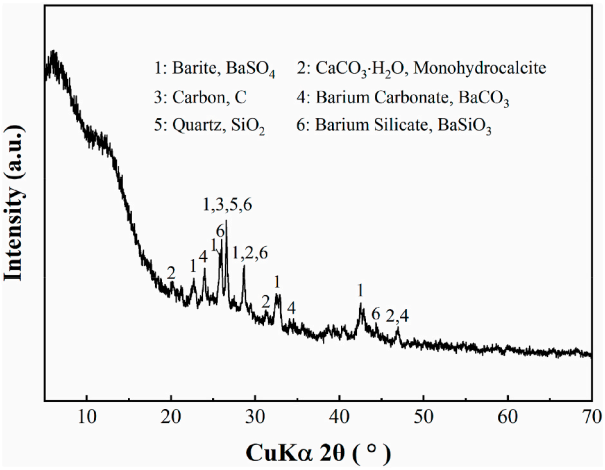

Fig. 1. XRD pattern of BS sample.

3. Results and discussion

3.1. Composition of BS

The chemical composition of BS determined by XRF is given in Table 1. It can be seen that BaO, SiO_2 and CaO were the dominant components in BS, and other constituents such as Al_2O_3, Fe_2O_3, and MgO, were no more than 5%. It is worth noting that BaO was as high as 34.8%. On one hand, the high amount of barium makes BS heavy when it is used or added in application of building materials such as wall bricks. On the other hand, barium in BS can be recycled as a secondary source. XRD analysis results of BS are shown in Fig. 1, and it can be inferred that the main forms of barium in BS were barite, barium carbonate and barium silicate. In addition, BS also contained some other mineral composition, such as monohydrocalcite, carbon and quartz. $BaSO_4$ was still the dominant phase in BS due to the insufficient reaction of the carbothermal reduction process. As barium sulfate has low solubility in water, acid and alkali solution (Lamb et al., 2013; Mahmoud et al., 2018), it is challenging to recycle barium resource from BS. DTPA is believed to be an effective agent to dissolve barium-containing phases from BS to separate and recycle barium, and the residue can be used in building materials. Additionally, DTPA also has strong complexing ability to calcium (Kowacz et al., 2009) due to the similar chemical properties of barium and calcium. Considering that the content of CaO in BS was as high as 11.2%, calcium dissolution behavior under different conditions was also investigated.

3.2. Effect of leaching parameters

3.2.1. DTPA concentration and liquid solid ratio

The effect of DTPA dosages (concentration and volume) on the dissolution rate of BS was firstly investigated. Experiments were performed at 80 °C for 300 min with a liquid solid ratio of 50 mL/g at different DTPA concentrations of 0.025–0.30 mol/L. The effect of DTPA concentration on the leaching efficiencies of barium and calcium are shown in Fig. 2a. The results show that the dissolution trends of barium and calcium were generally consistent. With the increasing of DTPA concentration, the dissolution of barium and calcium increased obviously and then slight decreases of leaching efficiency were observed after reaching the maximum value. Specifically, as the DTPA concentration increased from 0.025 to 0.10 mol/L, the leaching efficiency of barium remarkably increased from 7.57% to 78.64%. The results could be explained by that the amount of DTPA molecule was insufficient for barium in BS when its concentration was less than 0.10 mol/L. However, as the concentration further increased to 0.30 mol/L, the barium leaching efficiency declined slightly to 74.88%. The most likely causes for this slight decrease could be that an effective contact between DTPA and BS particles was reduced. There are several researches concerned on this phenomenon (Putnis et al., 2008; Bageri et al., 2017b; Abib et al., 2018). Superfluous DTPA may cause a shielding layer formation on the particle surfaces interfering in the effective contact (Abib et al., 2018). The increasing DTPA concentration will result in that carboxylate functional groups of DTPA aggregate on the particle surfaces (Kowacz et al., 2009; Abib et al., 2018), reducing the surfaces to effectively contact the solution. Meanwhile, Kowacz et al. (2009) pointed out that the ionization degree of DTPA would be reduced at a high concentration level leading to the decrease of leaching efficiency. The previous literature (Bageri et al., 2017b) also indicated that when the concentration increased to be more than 20% of DTPA (approximately equal to 0.5

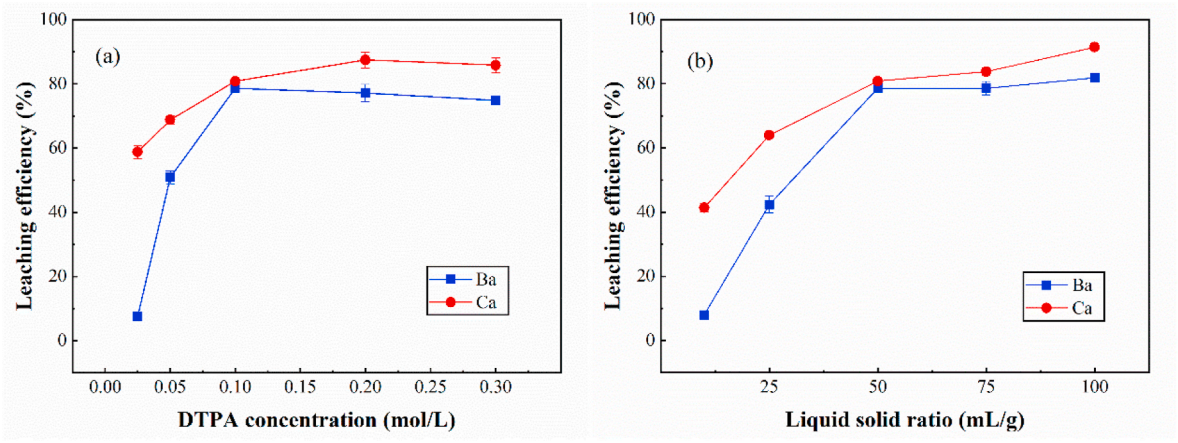

Fig. 2. The effects of DTPA dosages on the Ba and Ca leaching efficiency. (a) DTPA concentration investigation at conditions of 50 mL/g, 80 °C, 300 min and pH 12.0. (b) Liquid solid ratio investigation at conditions of 0.1 mol/L, 80 °C, 300 min and pH 12.0.

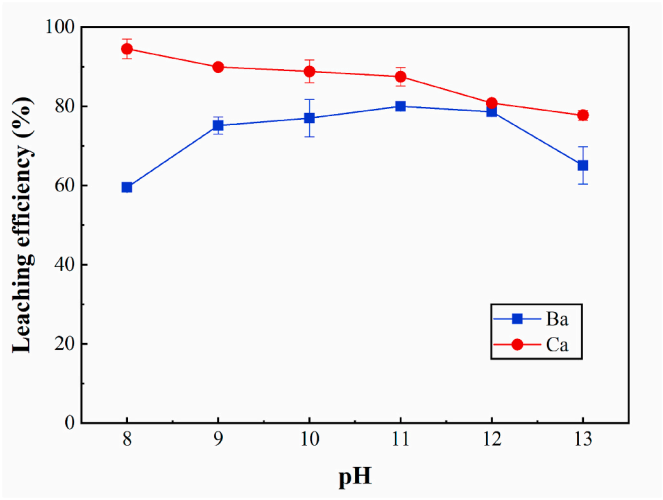

Fig. 3. Effect of pH on the leaching efficiencies of Ba and Ca under the conditions of using 0.10 mol/L DTPA at 80 °C for 300 min with a liquid solid ratio of 50 mL/g.

mol/L), the viscosity will rise and the reaction will be retarded. Therefore, the DTPA concentration of 0.10 mol/L was selected as the optimum condition for the dissolution of barium from BS used in this study.

Considering calcium in BS accounts for high content and calcium can also be complexed in DTPA solution, the dissolution behavior of calcium was also discussed. Totally, the dissolution rates of calcium from BS were slightly higher than those of barium under the same conditions. The maximum calcium leaching rate reached 87.48% at the DTPA concentration of 0.20 mol/L. It has been widely reported that DTPA has greater complexing ability for calcium ions than for barium ions (Kowacz et al., 2009; Abdelgawad et al., 2019; Thakur et al., 2021), and that calcium can form stronger complexes with the DTPA than barium (Thakur et al., 2021). Due to this reason, the higher affinity of calcium with DTPA resulted in the higher leaching efficiencies in comparison to barium as shown in Fig. 2a. However, in the leachate of this study, barium ions are the dominant ions because barium oxide in the BS is three times the content of calcium oxide.

The previous stage revealed that the DTPA concentration can affect the leaching rate, but to increase the leaching efficiency of barium cannot depend entirely on the rising concentration. At the same concentration, the volume of DTPA may play a major role in the leaching process, so the effect of the liquid solid ratio on leaching efficiency was investigated. In this trial, each 2.0 g BS sample was leached using 0.1 mol/L DTPA (at pH 12.0) solutions with different liquid solid ratios at 80 °C for 300 min. The effect of the liquid solid ratio on leaching efficiencies of barium and calcium are shown in Fig. 2b. It is shown that the dissolution efficiencies of barium and calcium increased with the increasing liquid solid ratio. A significant improvement of barium/calcium leaching efficiency was observed when the liquid solid ratio increased to 50 mL/g. Further increasing the liquid solid ratio to 100 mL/g, barium and calcium leaching efficiencies could be 81.84 and 91.41%, respectively. These results implied that barium/calcium leaching efficiency depended on the volume used when the liquid solid ratio was no more than 50 mL/g, and a leaching balance of barium/calcium was observed from the liquid solid ratio of 50–100 mL/g. Similar results were also identified by Putnis et al. (1995) involving the dissolution efficiency of barium sulfate scale with DTPA-base solvent. Although the liquid solid ratio of 100 mL/g could obtain higher dissolution efficiencies, the increase of barium dissolution efficiencies was insignificant compared with the liquid solid ratio to 50 mL/g. Considering that the high volume will cause a cost burden, the liquid solid ratio of 50 mL/g was suggested as the optical react condition.

3.2.2. *Effect of system pH value*

Aside from chelate concentrations and volumes, pH is also one of the main factors for the barium dissolution using DTPA solution. The effect of pH on the leaching efficiencies of barium and calcium is displayed in Fig. 3. It can be seen that the dissolution trends of barium and calcium were inconsistent especially at the pH range of 8.0–11.0. Calcium totally exhibited a declining dissolution rate as the system pH increased. Hydroxide ions concentrations increased with pH increasing, and the increasing hydroxide ions can compete with the DTPA chelating agent for the calcium ions (Fredd and Fogler, 1998). This might be the main reason for a decline of the calcium leaching efficiency. The barium leaching efficiency increased from 59.52 to 80.00% while the solution pH varied from 8.0 to 11.0. The results can be explained by that the complexing ability of DTPA with barium was reduced for hydrogen ions occupy a partially coordinated functional group with pH declined from 11.0 to 8.0 (Bageri et al., 2017a). Meanwhile, it was observed that the dissolution of barium exhibited a small degree of inhibition as pH further changed from 12.0 to 13.0. The decline tendency was also descried in the previous literatures (Li et al., 2016; Bageri et al., 2017b). However, hydroxide ions competition effect cannot explain the decline leaching efficiency of barium for barium hydroxide is soluble, which is different from calcium hydroxide. Similar results were obtained by Bageri et al. (2017b), and the reason was not clearly stated.

It can be concluded that the optimum pH for barium dissolution differs from that of calcium especially while the pH decreases from 11.0 to 8.0. The results are important for barium dissolution from BS and are

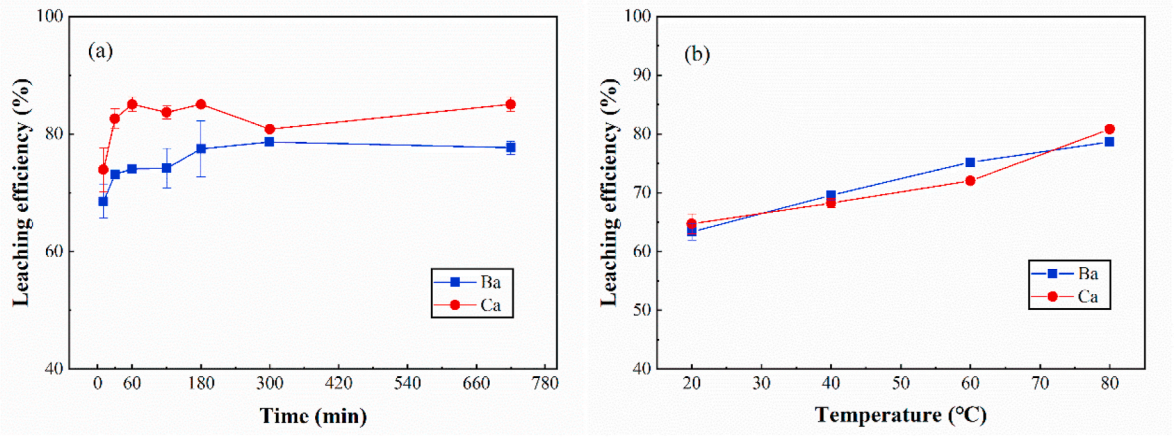

Fig. 4. Effect of (a) leaching time and (b) reaction temperature on the leaching efficiencies of Ba and Ca under the conditions of 0.10 mol/L DTPA solution (pH = 12.0) with a liquid solid ratio of 50 mL/g.

indicative for barium releasing from DTPA complex solution. On one hand, pH of 12.0 was selected for selectively leaching barium, in which condition barium had a relatively higher leaching rate while calcium had a relatively lower one. Although DTPA solution has stronger complexing ability for calcium ions than for barium ions (Kowacz et al., 2009), barium dissolution efficiency (78.64%) which was close to calcium (80.84%) was realized when the pH was set at 12.0. On the other hand, the complexation capacity differences between Ba-DTPA and Ca-DTPA tend to be widened as the pH decreases as shown in Fig. 3. Therefore, to decline pH of the DTPA complex solution from 12.0 to 8.0 or less, Ba-DTPA is expected to decomplex prior to Ca-DTPA. This is the basis to separate calcium from the DTPA complex solution to obtain barium sulfate products.

3.2.3. Leaching time and temperature

The leaching time experimental investigation of BS was performed with the reaction time from 10 to 720 min using 0.10 mol/L DTPA with pH of 12.0 at 80 °C, the liquid solid ratio of 50 mL/g. The results are shown in Fig. 4a, and it indicated that as the reaction time went on, the dissolution of barium and calcium increased gradually and then achieved saturated values. When the reaction lasted for 300 min, the reaction approximately reached equilibrium, and the dissolution rate almost no longer increased. At equilibrium, the leaching efficiencies of barium and calcium can be up to 78.64% and 80.84%, respectively.

To investigate the effect of temperature on barium leaching efficiency, the leaching experiment was carried out at various temperatures using 0.10 mol/L DTPA with pH of 12.0 for 300 min, the liquid solid ratio of 50 mL/g. The results are shown in Fig. 4b. It can be seen that the leaching efficiencies of barium and calcium ions increased with increasing temperature. As the temperature increased from 20 to 80 °C, the dissolution rates of barium and calcium respectively increased from 63.34 to 78.64% and from 64.73 to 80.84%. The results have demonstrated that DTPA is more effective in high temperatures. At higher temperatures, the diffusion rate of water molecules is faster, and the ionization constant of DTPA is higher, which assists the dissolution of barium (Kowacz et al., 2009). Based on the analysis of the above results, the optimal leaching conditions were using 0.10 mol/L DTPA (pH = 12.0) at 80 °C for 300 min with a liquid solid ratio of 50 mL/g. The residue remaining under this condition is mainly composed of quartz and carbon, which is expected to be further applied in building materials (Fig. S2).

3.3. Synthesis of $BaSO_4$ particles from mixed complexation solution

3.3.1. Decomplexation of Ba-DTPA

Barium in chelating agent solutions, such as sodium hexametaphosphate (Gupta et al., 2010), polycarboxylate (Saraya and Bakr, 2011), sodium polyacrylate (Sun et al., 2013), and EDTA (Hu et al., 2015), can be released through decomplexation methods. However, seldom work focus on the behavior of barium decomplexation from Ba-DTPA solution, especially from the Ca- and Ba-mixed complexation solution. As discussed, barium and calcium in BS were both dissolved in DTPA solution. To investigate the selective releasing behavior of barium from the Ba-DTPA and Ca-DTPA solution, chemical reagent should be added to destroy the complex structure. It has been reported that SO_4^{2-} would release and enter into the solution while complexing dissolution of $SrSO_4$ occurred to form Sr-DTPA using DTPA solution (Coll de Pasquali et al., 2019). In this work, as barium and calcium were complexed with DTPA to form Ba-DTPA and Ca-DTPA solution, their corresponding anions, mainly SO_4^{2-}, also released and presented as dissolved states in the solution. In theory, when using mineral acids to adjust the solution pH, Ba-DTPA complex would slowly dissociate and release barium ions to form $BaSO_4$ particles finally.

Ba-DTPA and Ca-DTPA solution obtained under the optimum conditions: 0.10 mol/L DTPA (pH 12.0) leaching BS at 80 °C for 300 min with a liquid solid ratio of 50 mL/g, was used to investigate the releasing behavior of barium and calcium. As shown in Fig. 3, the complexing stability of Ba-DTPA decreased with decreasing pH from 11.0 to lower. To adjust the solution pH, 2 mol/L of H_2SO_4 and HCl solutions were respectively added to lower the pH to 7.5. The results showed that the particle size of the $BaSO_4$ product obtained using HCl was greater than that of using H_2SO_4 (Fig. S1). Importantly, the yield of the product obtained using HCl was one-third of that of using H_2SO_4. These could be assigned to the fact that sulfate ions in the solution were insufficient to precipitate the releasing barium ions when using HCl to adjust the system pH. By contrast, only using Na_2SO_4 solution (1 mol/L) can provide enough sulfates in the solution, but no $BaSO_4$ precipitate was obtained due to the unchanged pH value. In view of this, sulfuric acid was suitable for barium decomplexation for it can lower the system pH and can provide sulfates to produce $BaSO_4$ particles through homogeneous precipitation. The possible reactions of barium complexation and decomplexation with DTPA can be summarized as the following equations:

$$Ba^{2+} + DTPA \xrightarrow{pH\ increase} Ba - DTPA \quad (2)$$

$$Ba - DTPA + SO_4^{2-} \xrightarrow{pH\ decrease} BaSO_4 + DTPA \quad (3)$$

To determine the decomplexation efficiency of barium ions at the acidifying process, the percentage of barium, calcium, and silicon (sillicon had a low leaching efficiency but its concentration in leachate solution was relatively high) in solution were calculated as listed in Table 2. When the Ba-DTPA and Ca-DTPA solution was acidified by 2 mol/L H_2SO_4, three critical points at pH of 9.0, 8.5 and 7.5 were observed. As pH turned from 12.0 to 9.0, solution turned to be cloudy. After filtering the $BaSO_4$ precipitate, 72.69% barium remained in the solution, which suggested that only a small amount of barium was displaced from the complex while DTPA still had strong complexing ability to barium. The precipitates obtained at pH of 9.0 had a low yield with the impurities of silicon inside. As the pH value decreased from 9.0 to 8.5, Ba-DTPA complex became destabilized and the solution turned into white pasty with precipitates gradually generated. The results showed that 90.46% of the barium was dissociated from the complexing state to form $BaSO_4$ precipitates, indicating most of the Ba-DTPA decomposed and simultaneously white precipitates appeared in the solution. With the solution being further acidified to 7.5 and lower, all of the barium ions (99.86%) were displaced from the complexs and the precipitates were no longer generated after 12 h. It can be clearly seen that most of the calcium was left in the solution, which can be attributed to the fact that Ca-DTPA is more difficult to decompose than Ba-DTPA complexes (Thiele et al., 2018). The results are also consistent with the phenomenon that DTPA solution has stronger complexing ability with calcium than with barium when pH decreased from 9.0 to lower as discussed in Fig. 3. The purity of $BaSO_4$ products obtained at pH of 8.5 and 7.5 were higher than 90% (Table S1). Meanwhile, calcium contents in the two $BaSO_4$ products were less than 0.2%, implying that calcium and barium have been well separated by the acidifying process.

After $BaSO_4$ precipitates were separated from the solution at pH of 7.5, the leachate was collected and re-adjusted to 12.0 for cycle leaching. Cycle leaching experiments of original BS were performed in triplicate at 80 °C for 300 min with a liquid solid ratio of 50 mL/g. The results are shown in Fig. S3, which indicated that DTPA cannot be recyclable well for barium leaching. This could be assigned to the fact that Ca-DTPA did not precipitate during the acidifying process and the

Table 2
The percentage of barium, calcium, and silicon in solution at different pH values adjusted using H_2SO_4 (wt %).

pH	9.0	8.5	7.5
Ba	72.69	9.54	0.14
Ca	97.50	88.19	88.99
Si	12.79	15.46	14.99

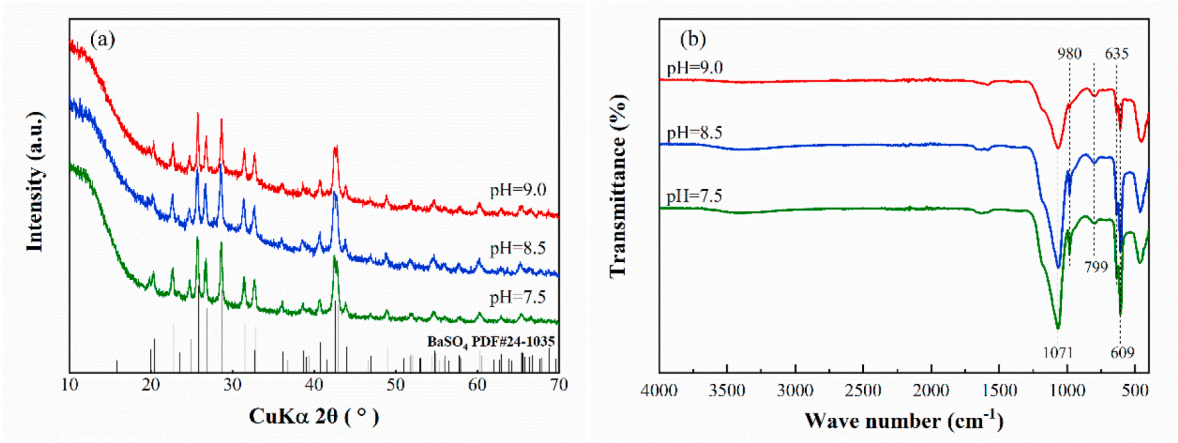

Fig. 5. (a) XRD patterns and (b) FTIR spectra of $BaSO_4$ particles obtained at different pH values.

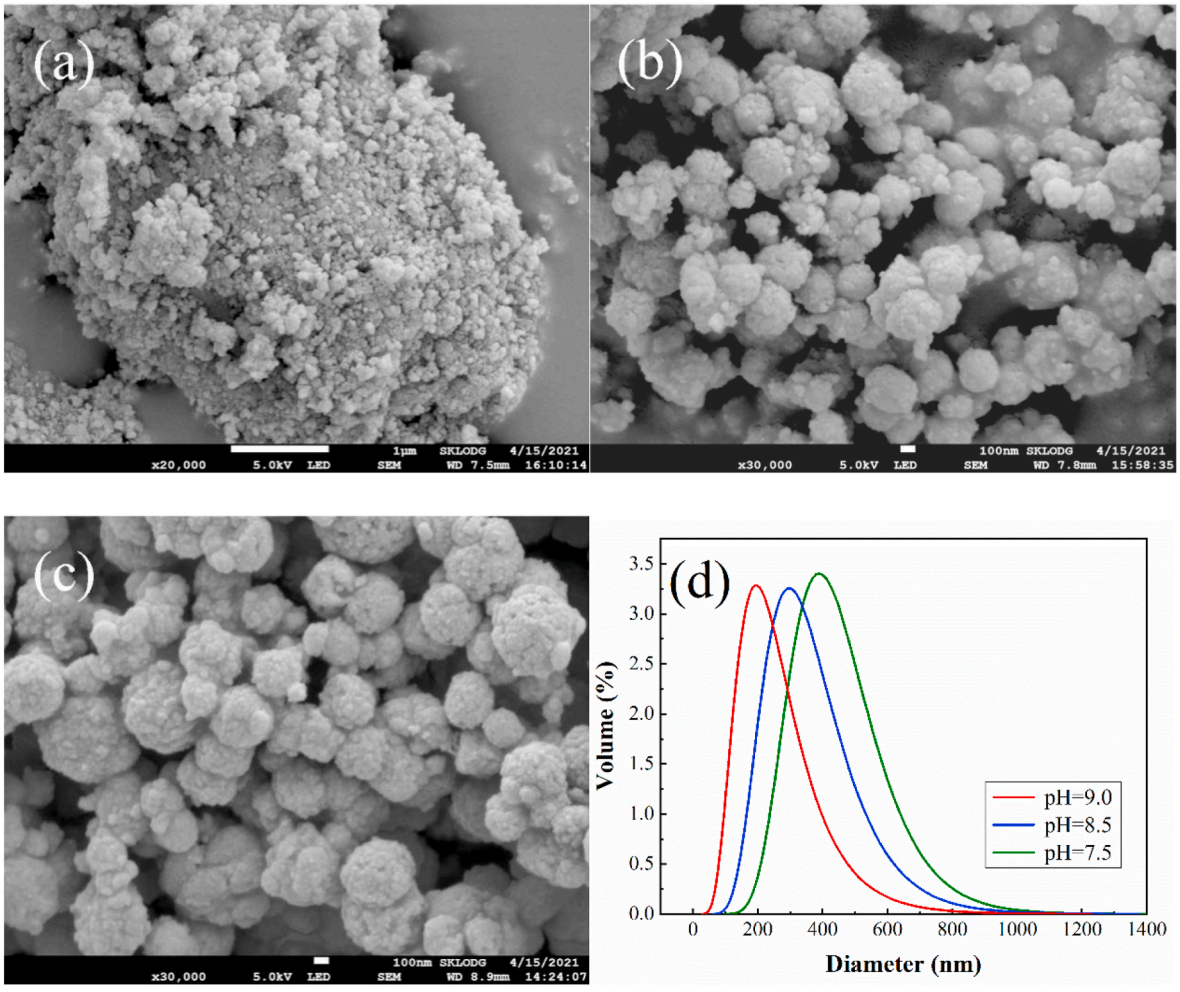

Fig. 6. SEM images of the $BaSO_4$ particles obtained at varying pH: (a) 9.0, (b) 8.5, (c) 7.5, and (d) the corresponding particle size distribution.

available DTPA became to be less. As discussed in Fig. 2a, calcium formed prior to barium for a low concentration of DTPA solution.

3.3.2. *Characterization of $BaSO_4$ particles*

XRD and FTIR were employed to identify the phase components and surface characteristics of precipitates obtained at different pH values adjusted by H_2SO_4. Fig. 5a shows the XRD patterns of the $BaSO_4$ powders. All the diffraction peaks of various materials were well consistent with the standard orthorhombic structure of $BaSO_4$ (PDF#24–1035). In addition, it can be noted that no impurity peaks were observed. There were no corresponding peaks of impurities in XRD patterns, probably due to the presence of silica in amorphous form. Likewise, as shown in FTIR results (Fig. 5b), the peaks at 1071 and 980 cm^{-1} were ascribed to the symmetric vibrational of SO_4^{2-}, while 609 and 635 cm^{-1} peaks corresponded to out-of-plane bending vibrational of SO_4^{2-} (Sun et al., 2013). All the above peaks of the spectra further confirmed the existence

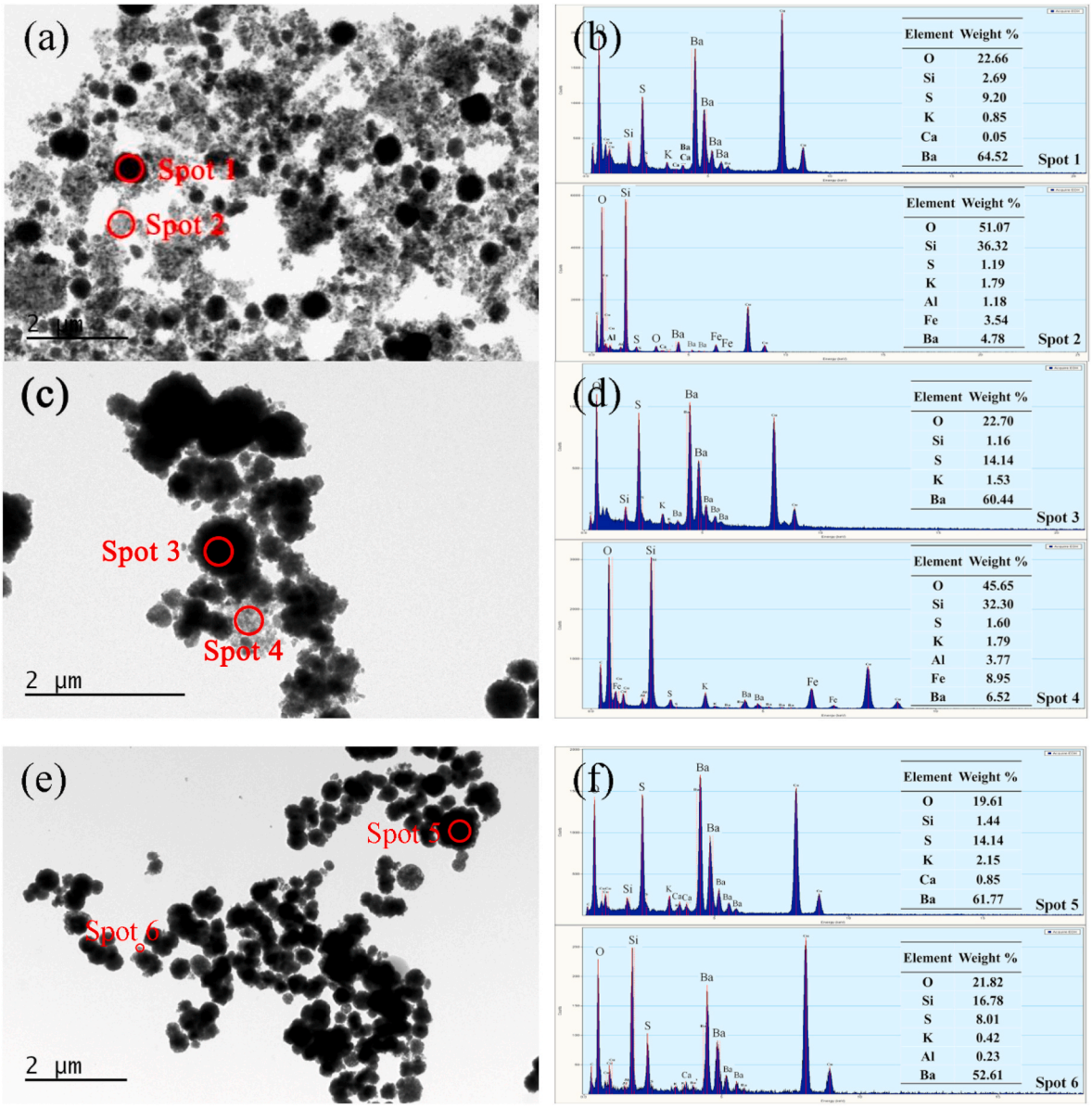

Fig. 7. TEM images and the corresponding EDS spectra of the $BaSO_4$ products obtained under different pH values. (a–b) pH of 9.0, (c–d) pH of 8.5, and (e–f) pH of 7.5.

of $BaSO_4$. It can also be seen that the spectra obtained at pH 9.0 slightly differs from the two others, reflecting in the weaker strength of the peaks assigned to $BaSO_4$. The absorption band at 799 cm^{-1} was attributed to Si–O–Si symmetric stretching vibration (Rafiee and Mehdizadeh, 2018), which revealed that the particles contain silica.

The morphology and size of the synthetic $BaSO_4$ products obtained at different pH were characterized by SEM and DLS. As observed in Fig. 6, the SEM images indicated that $BaSO_4$ products obtained at pH of 9.0 (Fig. 6a) were aggregation comprised of fine irregular particles, while the products obtained at pH of 8.5 and 7.5 (Fig. 6b and c) were nearly spherical shapes with average diameters of 300–500 nm. It also can be observed that the sizes of barium sulfate products obtained at pH of 8.5 are greater than those obtained at pH of 7.5. These findings were also verified by the DLS results as shown in Fig. 6d. When the pH was 9.0, the releasing yield of barium was low and diluted solution can grow fine barium sulfate crystals. With pH declining, the complex of Ba-DTPA became less stable and more free barium ions entered into the solution resulting in a saturation system to produce larger particles (Liu et al., 2018). The size distribution analysis results exhibited that the average diameter of three products obtained at pH of 9.0, 8.5 and 7.5 were respectively 331.73, 426.44 and 500.58 nm. These results of DLS agreed with the particle size obtained from the SEM analysis.

Fig. 7 presents the TEM-EDS analysis to further reveal the surface microstructure and corresponding element composition of the $BaSO_4$ products. TEM-EDS analysis discriminated the impurities in the $BaSO_4$ products, especially the ones obtained at pH of 9.0 (as shown in Fig. 7a and b). The gray flocculent substances were demonstrated to be impurities of silicon oxide, while the black spherical materials are $BaSO_4$ particles. It can be seen that gray flocculent substances decreased with the decreasing pH value. There was 85–88% of silicon that precipitated in products as impurities at different pH values as shown in Table 2. The silicon contents in products obtained at pH of 8.5 and 7.5 (Fig. 7c–d and e-f) were less than that in the product obtained at pH of 9.0 for more $BaSO_4$ was precipitated with pH decreasing.

4. Conclusions

In the current study, DTPA was used to investigate the dissolution behavior of BS under different conditions. The results demonstrated that DTPA can effectively dissolve barium from BS. The concentration and volume of DTPA can affect leaching efficiencies of the barium. As the DTPA concentration changed from 0.025 to 0.10 mol/L, the barium leaching efficiency increased from 7.57% to 78.64%. The optimum experimental conditions for leaching barium form BS were recommended as using 0.10 mol/L DTPA with pH of 12.0 at 80 °C for 300 min, and the liquid solid ratio of 50 mL/g. Meanwhile, submicron $BaSO_4$ particles have been synthesized successfully from Ba-DTPA leachates by acidifying using H_2SO_4. At pH of 9.0, $BaSO_4$ precipitation started, and the precipitation finished as the pH was at 7.5. The $BaSO_4$ products obtained at pH of 7.5 had an ellipsoidal structure with the average particle sizes of approximately 500 nm.

CRediT authorship contribution statement

Tengfei Guo: Investigation, Resources, Data curation, Writing – original draft. **Hannian Gu:** Writing – review & editing, Conceptualization, Validation, Resources, Methodology, Supervision, Funding acquisition. **Ning Wang:** Conceptualization, Resources, Supervision.

Declaration of competing interest

The authors declare that they have no known competing financial interests or personal relationships that could have appeared to influence the work reported in this paper.

Acknowledgments

The work was financially supported by the National Natural Science Foundation of China (U1812402), The Youth Innovation Promotion Association CAS (2021400), and Guizhou Outstanding Young Scientific and Technological Talents Project (2021–5641). Authors are grateful to Prof. Wan's Group for FTIR and DLS determination.

Appendix A. Supplementary data

Supplementary data to this article can be found online at https://doi.org/10.1016/j.jclepro.2022.132482.

References

Abdelgawad, K., Mahmoudet, M., Elkatatny, S., Patil, S., 2019. Effect of calcium carbonate on barite solubility using a chelating agent and converter, 193566 SPE International Conference on Oilfield Chemistry 1–10.
Abib, G.A.P., Da Cruz, G.F., Vaz Junior, A.S.L., 2018. Study of barium sulfate dissolution by scale dissolver based on solutions of DTPA. An. Acad. Braz. Ciênc. 90, 3185–3196.
Bageri, B.S., Mahmoud, M., Abdulraheem, A., Al-Mutairi, S.H., Elkatatny, S.M., Shawabkeh, R.A., 2017a. Single stage filter cake removal of barite weighted water based drilling fluid. J. Petrol. Sci. Eng. 149, 476–484.
Bageri, B.S., Mahmoud, M.A., Shawabkeh, R.A., Abdulraheem, A., 2017b. Evaluation of barium sulfate (barite) solubility using different chelating agents at a high temperature. J. Petrol. Sci. Technol. 7, 42–56.
Chen, P., Ma, B., Tan, H., Liu, X., Zhang, T., Li, C., Yang, Q., Luo, Z., 2021. Utilization of barium slag to improve chloride-binding ability of cement-based material. J. Clean. Prod. 283, 124612.
Coll de Pasquali, D., Horai, E., Real, M.I., Castro, S., Dunn, F.B., Gunawan, G., Azam, H. M., Wilson, J.M., 2019. Chemical dissolution of oilfield strontium sulfate ($SrSO_4$) scale by chelating agents. Appl. Geochem. 106, 134–141.
Ding, J., 2005. Using barium slag processing wastewater containing chromium (VI). Environ. Prot. Chem. Ind. 25, 225–227 (In Chinese).
Dong, C., Chen, Y., Wang, Y., 2003. Comprehensive utilization of barium containing waste residue. Hebei Chem. Eng. Ind. 5, 53–54 (In Chinese).
Dunn, K., Yen, T.F., 1999. Dissolution of barium sulfate scale deposits by chelating agents. Environ. Sci. Technol. 33, 2821–2824.
Fredd, C.N., Fogler, H.S., 1998. The influence of chelating agents on the kinetics of calcite dissolution. J. Colloid Interface Sci. 204, 187–197.
Gu, H., Guo, T., Dai, Y., Wang, N., 2019. Non-hazardous treatment for barium slag using phosphogypsum. Waste Biomass Valori 10, 3157–3161.
Guo, T., Gu, H., Ma, S., Wang, N., 2020. Increasing phosphate sorption on barium slag by adding phosphogypsum for non-hazardous treatment. J. Environ. Manag. 270, 110823.
Gupta, A., Singh, P., Shivakumara, C., 2010. Synthesis of $BaSO_4$ nanoparticles by precipitation method using sodium hexa metaphosphate as a stabilizer. Solid State Commun. 150, 386–388.
Guzmán, D., Fernández, J., Ordoñez, S., Aguilar, C., Rojas, P.A., Serafni, D., 2012. Effect of mechanical activation on the barite carbothermic reduction. Int. J. Miner. Process. 102–103, 124–129.
He, W., Li, R., Zhang, Y., Nie, D., 2022. Synergistic use of electrolytic manganese residue and barium slag to prepare belite- sulphoaluminate cement study. Construct. Build. Mater. 326, 126672.
Hu, L., Wang, G., Yang, C., Cao, R., 2015. Fabrication of submicron barium sulfate aggregates in the presence of ethylenediaminetetraacetic acid anions. Particuology 22, 157–162.
Huang, X., Xin, C., Li, J.-S., Wang, P., Liao, S., Poon, C.S., Xue, Q., 2022. Using hazardous barium slag as a novel admixture for alkali activated slag cement. Cement Concr. Compos. 125, 104332.
Jamshidi, E., Ale Ebrahim, H., 2008. A new clean process for barium carbonate preparation by barite reduction with methane. Chem. Eng. Process 47, 1567–1577.
Jiang, R., 2007. Study of barium slag gelling and activating property and application. Coal Ash China 19, 24–26 (In Chinese).
Kowacz, M., Putnis, C.V., Putnis, V., 2009. The control of solution composition on ligand-promoted dissolution: DTPA-Barite Interactions. Cryst. Growth Des. 9, 5266–5272.
Lamb, D.T., Matanitobua, V.P., Palanisami, T., Megharaj, M., Naidu, R., 2013. Bioavailability of barium to plants and invertebrates in soils contaminated by barite. Environ. Sci. Technol. 47, 4670–4676.
Li, N., He, D., Zhao, L., Liu, P., 2016. An alkaline barium- and strontium-sulfate scale dissolver. Chem. Technol. Fuels Oils 52, 16–20.
Liu, L., Jia, S., Wang, Y., Chen, Y., Zhang, Q., Yang, L., 2017. Study on application of barium residue in building materials and effect of heavy metal curing. Brick-Tile 5, 25–27 (In Chinese).
Liu, Y., Guo, X., Yang, S., He, G., Jin, H., 2018. Controllable preparation of uniform micron-sized barium-sulfate spheres. Cryst. Res. Technol. 53, 1700212.
Lu, Q., Xu, X., Liang, L., Xu, Z., Shang, L., Guo, J., Xiao, D., Qiu, G., 2019. Barium concentration, phytoavailability, and risk assessment in soil-rice systems from an active barium mining region. Appl. Geochem. 106, 142–148.
Mahmoud, M., Bageri, B., Abdelgawad, K., Kamal, M.S., Hussein, I., Elkatatny, S., Shawabkeh, R., 2018. Evaluation of the reaction kinetics of DTPA chelating agent and converter with barium sulfate (Barite) using rotating disk apparatus. Energy Fuel. 32, 9813–9821.
Menzie, C., Southworth, B., Stephenson, G., Feisthauer, N., 2008. The Importance of understanding the chemical form of a metal in the environment: the case of barium sulfate (barite). Hum. Ecol. Risk Assess. 14, 974–991.
Mulopo, J., Motaung, S., 2014. Carbothermal reduction of barium sulfate-rich sludge from acid mine drainage treatment. Mine Water Environ. 33, 48–53.
Putnis, A., Putnis, C.V., Paul, J.M., 1995. The efficiency of a DTPA-Based solvent in the dissolution of barium sulfate scale deposits, 029094 SPE International Symposium on Oilfield Chemistry 773–785.
Putnis, C.V., Kowacz, M., Putnis, A., 2008. The mechanism and kinetics of DTPA-promoted dissolution of barite. Appl. Geochem. 23, 2778–2788.
Rafiee, F., Mehdizadeh, N., 2018. Palladium N-Heterocyclic carbene complex of vitamin B_1 supported on silica-coated Fe_3O_4 nanoparticles: a Green and efficient catalyst for C-C coupling. Catal. Lett. 148, 1345–1354.
Salem, A., Jamshidi, S., 2012. Effect of paste humidity on kinetics of carbothermal reduction of extruded barite and coke mixture. Solid State Sci. 14, 1012–1017.
Salem, A., Osgouei, Y.T., 2009. The effect of particle size distribution on barite reduction. Mater. Res. Bull. 44, 1489–1493.
Saraya, M.E.S.I., Bakr, I.M., 2011. Synthesis of $BaSO_4$ nanoparticles by precipitation method using polycarboxylate as a modifier. Am. J. Nanotechnol. 2, 106–111.
Shang, F., Su, X., Shang, S., 2021. Study on recovery of barium from barium slag by chlorination roasting-water leaching process. Inorganic Chemicals Industry 53, 65–67 (In Chinese).
Sun, Y., Zhang, F., Wu, D., Zhu, H., 2013. Roles of polyacrylate dispersant in the synthesis of well-dispersed $BaSO_4$ nanoparticles by simple precipitation. Particuology 14, 33–37.
Thakur, P., Ward, A.L., González-Delgado, A.M., 2021. Optimal methods for preparation, separation, and determination of radium isotopes in environmental and biological samples. J. Environ. Radioact. 228, 106522.
Thiele, N.A., MacMillan, S.N., Wilson, J.J., 2018. Rapid dissolution of $BaSO_4$ by Macropa, an 18-Membered macrocycle with high affinity for Ba^{2+}. J. Am. Chem. Soc. 140, 17071–17078.
Vaidya, R., Kodam, K., Ghole, V., Surya, M.R.K., 2010. Validation of an in situ solidification/stabilization technique for hazardous barium and cyanide waste for safe disposal into a secured landfill. J. Environ. Manag. 91, 1821–1830.
Xie, Y., Sun, Z., Han, T., Xie, Z., Zhang, J., Sun, H., Xiao, J., Wang, Y., Yu, F., Yang, N., 2021. Highly efficient utilization of industrial barium slag for carbon gasification in direct carbon solid oxide fuel cells. Int. J. Hydrogen Energy 46, 37029–37038.
Yang, T., Wang, N., Gu, H., Guo, T., 2021. Froth flotation separation of carbon from barium slag: recycling of carbon and minimize the slag. Waste Manag. 120, 108–113.
Zhu, J., Chen, Y., Zhang, L., Guo, B., Fan, G., Guan, X., Zhao, R., 2021. Revealing the doping mechanism of barium in sulfoaluminate cement clinker phases. J. Clean. Prod. 295, 126405.